

Predicting the Temperature Dependence of Surfactant CMCs Using Graph Neural Networks

Christoforos Brozos^{a,b}, Jan G. Rittig^b, Sandip Bhattacharya^a, Elie Akanny^a, Christina Kohlmann^a,
Alexander Mitsos^{d,b,c,*}

^a BASF Personal Care and Nutrition GmbH, Henkelstrasse 67, 40589 Duesseldorf, Germany

^b RWTH Aachen University, Process Systems Engineering (AVT.SVT), Aachen, Germany

^c Forschungszentrum Jülich GmbH, Institute for Energy and Climate Research IEK-10: Energy Systems Engineering, Jülich, Germany

^d JARA-ENERGY, Aachen, Germany

Abstract

The critical micelle concentration (CMC) of surfactant molecules is an essential property for surfactant applications in industry. Recently, classical QSPR and Graph Neural Networks (GNNs), a deep learning technique, have been successfully applied to predict the CMC of surfactants at room temperature. However, these models have not yet considered the temperature dependency of the CMC, which is highly relevant for practical applications. We herein develop a GNN model for temperature-dependent CMC prediction of surfactants. We collect about 1400 data points from public sources for all surfactant classes, i.e., ionic, nonionic, and zwitterionic, at multiple temperatures. We test the predictive quality of the model for following scenarios: i) when CMC data for surfactants are present in the training of the model in at least one different temperature, and ii) CMC data for surfactants are not present in the training, i.e., generalizing to unseen surfactants. In both test scenarios, our model exhibits a high predictive performance of $R^2 \geq 0.94$ on test data. We also find that the model performance varies by surfactant class. Finally, we evaluate the model for sugar-based surfactants with complex molecular structures, as these represent a more sustainable alternative to synthetic surfactants and are therefore of great interest for future applications in the personal and home care industries.

1 Introduction

Surfactants are used in a wide variety of industries such as cosmetics, food additives, detergents, oil recovery, and pharmaceuticals due to their unique properties (Vieira et al., 2021; Shaban et al., 2020; Nitschke and Costa, 2007; Tadros, 2005; Adu et al., 2020; Szűts and Szabó-Révész, 2012; Massarweh and Abushaikh, 2020). Surfactants are amphiphilic molecules containing hydrophilic (head) and hydrophobic (tail) parts. A surfactant property of major interest is the critical micelle concentration (CMC), which is the concentration above which self-aggregation into micelles takes place and is highly relevant in many applications (Su et al., 2020; Thompson et al., 2023; Ghezzi et al., 2021; Kumar and Mandal, 2019). The CMC is accompanied by sharp changes in the bulk solution properties (Rosen and Kunjappu, 2012; Myers, 2020).

The influence of temperature on CMC is of great importance in surfactant applications, such as washing and oil recovery. Specifically, the CMC is influenced by multiple parameters that are related to the surfactant itself, such as the structure of the tail and nature of the head group, and parameters related to the solute environment, such as pH, temperature, and the presence of electrolytes (Rosen and Kunjappu, 2012; Myers, 2020; Katritzky et al., 2008; Thiruvengadam et al., 2020). The temperature is of particular interest, since no model applicable to all surfactant classes is available in the literature. Many researchers have studied the temperature effect on the CMC, which in general has been described as complex and varies for each surfactant class (Rosen and Kunjappu, 2012; Myers, 2020). For nonionics, authors have reported that CMC decreases monotonically as the temperature increases (Lindman et al., 2016), but in general C_iE_j (polyethylene oxide) type of surfactants exhibit a minimum CMC at temperature around 50°C (Rosen and Kunjappu, 2012; Myers, 2020; Kroll et al., 2022; Chen et al., 1998). In contrast, MEGA (N-alkanoyl-N-methylglucamide) surfactants show a U-shaped relationship (Prasad et al., 2006; Okawauchi et al., 1987). Ionic surfactants normally exhibit a U-shaped relationship too, with their minimum CMC value being between 20-30°C (Rosen and Kunjappu, 2012; Perger and Bešter-Rogač, 2007; Fu et al., 2019). It has been recently shown by Brinatti et al. (2014) that increasing the

* Corresponding author, E-mail: amitsos@alum.mit.edu

temperature causes a decrease in the CMC of some zwitterionics and others to exhibit a minimum CMC. The latter is also shown in the work of Mukerjee and Mysels (Mukerjee and Mysels, 1971). All the above are experimental observations for individual surfactants, but no model for explicit CMC predictions at multiple temperatures of a wide spectrum of surfactants has been derived. This leads to limitations in predicting the temperature-dependent CMC of new surfactant molecules and highlights the need to consider the surfactant structure in the development of predictive models.

Both bio-based surfactants and biosurfactants are of particular interest in personal and home care industries since they enable a transition from fossil to renewable feedstocks (Farias et al., 2021; Jahan et al., 2020). In the literature, biosurfactants are defined as those produced by biotechnology while bio-based surfactants are surfactants comprised of sustainable 100% natural-based feedstocks (Drakontis and Amin, 2020). Both bio-based surfactants and biosurfactants contain sugar-based groups, hence are also referred to as sugar-based surfactants. The general structure comprises a polar carbohydrate, like glucose, as the hydrophilic part and an alkyl chain as the hydrophobic part (Ruiz, 2008). Gaudin et al. (2019) recently discussed the impact of this chemical structure on the sugar-based surfactant properties. Specifically, they state that the CMC can be affected by the stereochemistry and the anomeric configuration of the sugar head. Although sugar-based surfactants belong to nonionics, the effect of temperature on their solution properties differs from the ethoxylated ones (Molina-Bolívar et al., 2004). Researches have reported a decrease in CMC with the increase of temperature (Molina-Bolívar et al., 2004) and a U-shaped relationship in other cases (Paula et al., 1995; Angarten and Loh, 2014; Castro et al., 2018), thus showing again a complex relationship between surfactant structure, CMC and temperature.

The importance of CMC as a key characteristic surfactant property has driven many researchers to investigate the relationship between surfactant structure and CMC (Rosen and Kunjappu, 2012). Empirical equations have been derived from experimental data to describe this relationship, but they are only applicable to specific systems (Rosen and Kunjappu, 2012; Klevens, 1953). Recently, numerous quantitative structure-property relationship (QSPR) type models were developed for CMC prediction (Katritzky et al., 2008; Gaudin et al., 2016; Hu et al., 2010; Mattei et al., 2013; Wang et al., 2018; Aboali and Soleimani, 2023; Seddon et al., 2022). In QSPR models, molecular descriptors are estimated from the molecular structure and mapped to the target property. One limitation is that they typically require manual selection and identification of effective molecular descriptors.

An alternative end-to-end deep learning approach, called graph neural networks (GNNs), has been successfully applied to numerous molecular property prediction tasks (Schweidtmann et al., 2020; Rittig et al., 2023a; Gilmer et al., 2017; Rittig et al., 2023b; Sanchez Medina et al., 2023, 2022; Yang et al., 2019). GNNs are applied directly to the molecular graph and extract the necessary structural information which they later use to predict the target property, thereby providing an end-to-end learning framework (Hamilton, 2020). Due to their broad success and adoption, GNNs have been effectively applied to predict the CMC and surface excess concentration (Γ_m) of surfactant monomers (Qin et al., 2021; Brozos et al., 2024; Moriarty et al., 2023). For both approaches, i.e., QSPR and GNNs, the temperature-dependency of CMC is rarely studied. In fact, the effect of the temperature on the CMC has only been modeled in one recently published QSPR model, which is however limited to anionic surfactants (Aboali and Soleimani, 2023). We therefore aim at investigating the prediction of the temperature effect on CMC for all common surfactant types namely ionic, nonionic, and zwitterionic classes.

In the present work, we develop a GNN model for predicting the temperature-dependent CMC of all surfactant classes. To train the models, we extend our database of CMC values at room temperature for different surfactant classes from our previous work by adding CMC measurements at various from publicly available sources (Brozos et al., 2024). The extended database contains around 1400 measurements from 492 unique surfactant molecules. We then develop a GNN model that learns to extract structural information from the surfactant molecules in a fixed-size vector, known as the molecular fingerprint, in which we concatenate the experimental temperature. The updated vector is then mapped to the measured CMC of the surfactant. We incorporate stereochemistry and anomeric configuration information into the molecular graph representation. We train and fine-tune our model on the newly constructed database. We then test our model to predict the temperature-dependent CMC of i) surfactant structures seen during training but at different temperatures, and ii) completely new surfactants, i.e., not seen during training. Furthermore, we particularly explore the temperature dependency of the CMC of sugar-based

Tab. 1. A description of the nature of the data set used in this paper. The number of surfactants per class in the complete data set and the test sets are listed.

	Full data set	Test sets	
		Different temperature	Distinct surfactant
Anionics	576	100	89
Nonionics	422	62	68
Cationics	291	49	50
Zwitterionics	88	16	11
Total data points	1,377	227	218

surfactants. We show that in both test cases, the GNN model provides accurate predictions.

The remainder of this work is constructed as follows: First a description of the collected data set and of the test sets is provided in Section 2. In Section 3, we present the concept of the GNN for predicting temperature-dependent CMCs. Subsequently, the predictive quality of the developed GNN model is presented, discussed, and compared with previous works in Section 4. Finally, we conclude this contribution in Section 5. The test data used for model evaluation is publicly available in our [GitHub repository](#) and the model architecture is presented in Section 3. The training data set and the trained models remain property of BASF and could be made available upon request.

2 Data set

2.1 Data set overview

We collected a data set of temperature-dependent CMC values for a variety of surfactants. Particularly, we extended the assembled CMC data set from our previous work ([Brozos et al., 2024](#)), to include CMC information at multiple temperatures for each molecule, when such data was available. In the data collection process, we prioritized CMC values measured through tensiometry and we excluded any duplicates. For those surfactants for which we did not find tensiometry data, we considered CMC values determined by conductometry, light scattering, refractive index and calorimetry. Each data point includes the CMC, the temperature, and the isomeric SMILES string of the surfactant, allowing to distinguish between different anomers, e.g., octyl- α/β -D-glycoside, and chiral centers in the sugar head, e.g., glucoside with galactoside ([Weininger, 1988](#)). In total our new data set consists of 1,377 data points, with 492 unique surfactant structures of which 227 structures were measured at least at two different temperatures. The minimum temperature of our data is 0°C and the maximum is 90°C. The temperature distribution of the data set is illustrated in Figure 1. A detailed statistical analysis of the CMC data can be found in the Appendix A, cf. Figure A9.

The different relationships in each surfactant classes between temperature and CMC discussed in Section 1 are also present in our data set. In Figure 2, six surfactant examples are illustrated. Specifically, the three ionic surfactants, namely S1, S5, and S6 exhibit a U-shaped relationship, as often is the case for ionic surfactants. The minimum CMC is between 30 and 40°C. An exception to the U-shaped relationship is S2, an ionic surfactant too, as an increase in temperature causes the CMC to increase too. Finally, the sugar-based nonionic surfactant S3 and the zwitterionic surfactant S4 exhibit a U-shaped relationship.

2.2 Data splits

We implement two types of data set splitting: i) *different temperature* – for testing the prediction accuracy of our model at new temperatures; ii) *distinct surfactant* – for testing the ability of our model to generalize to new, unseen surfactant structures, hence structures not included in the model training at all. We note that the two test sets have a similar surfactant class distribution in Table 1, which was not enforced.

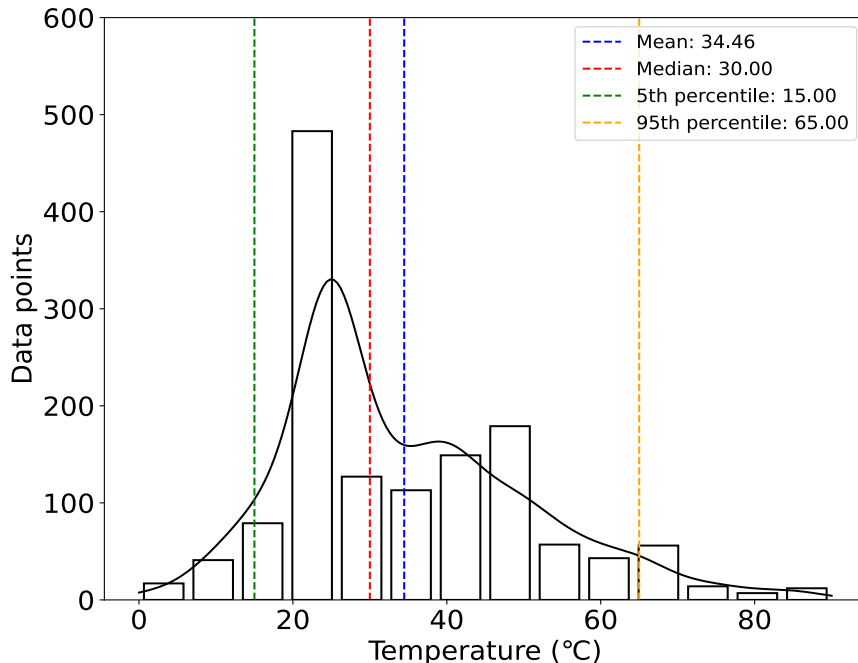


Fig. 1. Distribution of the CMC data with the number of data points over the temperature range of $T=10-90$ for a bin size of 10°C .

For selecting the *different temperature* test set, we first identify all unique surfactant molecules with CMCs in at least two different temperatures, and then randomly select one data point for each of these molecules to be in the test set. For example, if for a given surfactant there exist 3 measurements at 3 different (distinct) temperatures in the full data set, one will be randomly assigned to the test set and the other two remain in the training set. A total of 227 molecules at various temperatures are selected for testing, which accounts for about 16% of the whole data set size.

The *distinct surfactant* test set aims to evaluate the models’ predictive performance for completely unseen surfactant molecules at various temperatures. For consistency in the performance comparison, we choose similar test set size, namely 218 data points. We randomly select molecules and add all corresponding data points to the test, such that the temperature-dependent CMC values of these molecules remain completely unseen during training. In this final test set, about 70% of the data points were molecules measured at different/multiple temperatures. For these molecules, we include all available CMC values measured at different temperatures in the test set. The remaining 30% of the test set are molecules measured only at one temperature. In total, 50 distinct surfactant structures are included in the test set.

3 Methods

In the following sections, we first present the structure of our GNN model and describe ensemble learning (Section 3.1). Then, we summarize the hyperparameter selection and training settings of our model (Section 3.2).

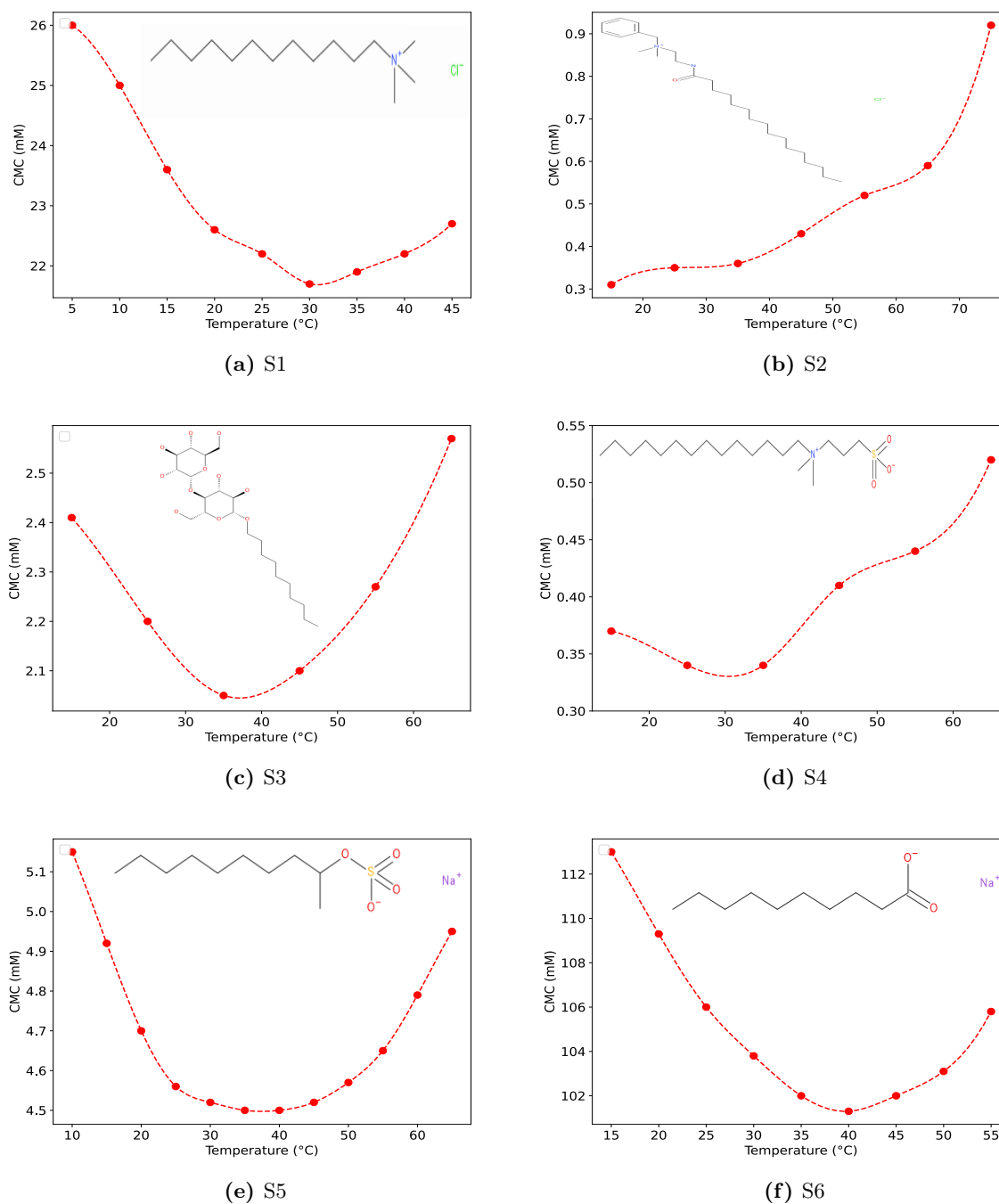


Fig. 2. Experimental values of CMC (in mM) at different temperatures for six surfactants present in our database are tabulated: (S1) dodecyltrimethylammonium chloride (DTAC) (Perger and Bešter-Rogač, 2007), (S2) benzyl (3-hexadecanoylaminoethyl)dimethylammonium chloride (C15AEtBzMe2Cl) (Galgano and El Seoud, 2010), (S3) Decyl diglucoside (Brinatti et al., 2014), (S4) Sulfobetaine 14 (Cheng et al., 2012), (S5) Sodium decyl 2 sulfate (Mukerjee and Mysels, 1971) and (S6) Sodium decanoate (González-Pérez et al., 2005). Each of these surfactants shows a different temperature dependence.

3.1 Graph Neural Networks and ensemble learning

We adapt our GNN model for predicting CMC values of surfactant monomers from our previous work (Brozos et al., 2024) to include the temperature dependency. An overview of the model framework is illustrated in Figure 3. The GNN takes as input a surfactant molecule, represented as an undirected molecular graph, where atoms correspond to nodes (vertices) and bonds to edges. Each node and each edge is assigned a feature vector, where chemical information about the corresponding atom/bond is stored. The node and edge features used in the current work are presented in Tables B5 and B6 respectively. GNNs operate directly on the node and edge features of the undirected molecular graph (Gilmer et al., 2017). During graph convolutions, the node features, denoted as hidden states, are updated with structural information from their neighborhood. Then, a pooling step is applied. That is, the updated hidden state of all nodes within the graph, which now contain information about the respective node itself and the neighbor nodes, are combined, e.g., by applying the sum operator, into a single unique vector representation, known as the molecular fingerprint. To include the temperature, we first normalized it between a minimum of 0 and a maximum of 10 and we concatenated the molecular fingerprint with it. Finally, the updated molecular fingerprint is used to perform the downstream property prediction task, herein predicting the CMC, in a standard multilayer perceptron (MLP). For a detailed overview of GNNs, including different types of graph convolutions and pooling operators we refer to works on graph convolutions layers (cf. (Hamilton et al., 2018; Veličković et al., 2018; Xu et al., 2019; Simonovsky and Komodakis, 2017)) and pooling operators (cf. (Cangea et al., 2018; Vinyals et al., 2016; Schweidtmann et al., 2023; Vu et al., 2023; Buterez et al., 2023)), also see reviews in (Zhou et al., 2020; Wu et al., 2021).

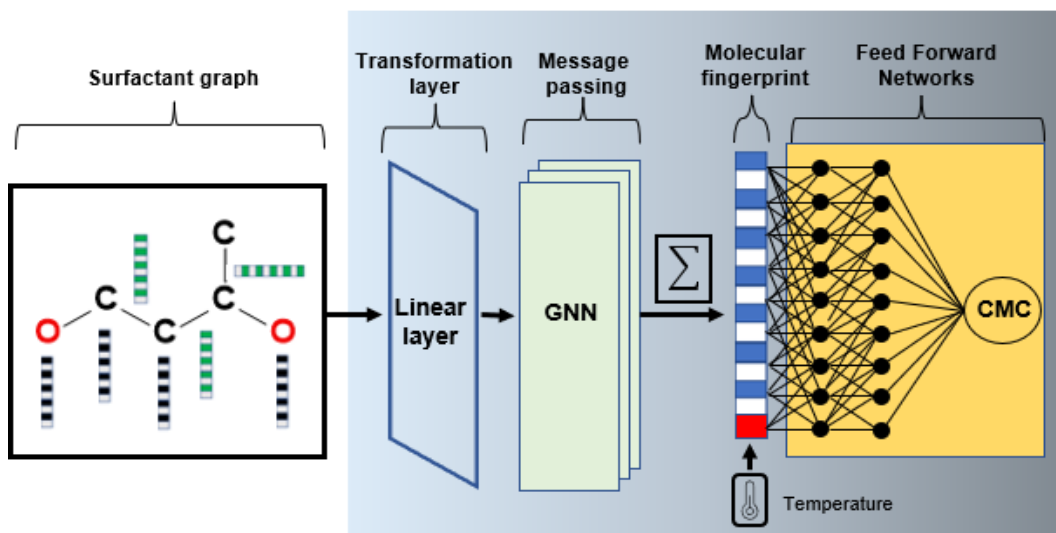


Fig. 3. Schematic representation of the developed graph neural network for predicting temperature-dependent CMC values of surfactant monomers.

In our previous work, we considered stereochemistry information on the edge feature vector (Brozos et al., 2024). As both chirality and stereochemistry of a surfactant molecule impact the CMC, we herein additionally use chirality information on the atom feature vector too. We note that more sophisticated approaches exist in the literature (Adams et al., 2021) and that using 3D information could be beneficial but requires to determine or calculate 3D coordinates and conformers which is computationally expensive. In our work, we aim to investigate whether the GNN model that learns from molecular graphs with chirality information can perform accurate predictions of CMC in different anomers and isomers too.

We further apply ensemble learning. Ensemble learning is a common technique in machine learning to reduce the noise of randomly chosen training and validation sets. Multiple models are trained, i.e., on different splits of training and validation sets, i.e., non-test data, and their predictions are averaged, thus leading to more robust and generalized predictions (Breiman, 1996; Dietterich, 2000; Ganaie et al., 2022). We herein train 40 different models on both split types mentioned in Section 2.2, and then we

average out the predictions to report the prediction accuracy of the ensemble of GNNs.

3.2 Implementation and hyperparameter

To determine the optimal hyperparameter values, we train our GNN model on 40 different seeded validation sets, similar to our previous works (Schweidtmann et al., 2020; Rittig et al., 2023a, 2022; Brozos et al., 2024). The size of the validation set is kept constant at 200 molecules, which represents about 14% of the whole data set size and thus a general training-validation-test split of 70:14:16. We use the *different temperature* test set for our hyperparameter tuning and we select the ones leading to the minimum root mean squared error (RMSE) on the validation set. We scale the CMC (μM) values using a (based 10) logarithmic scale. We use a grid search to investigate the hyperparameters of the GNN model described in Table B7. Note that the first layer of the MLP has a size of 129 neurons because we are concatenating the normalized temperature on the molecular fingerprint

We represent each surfactant molecule with an isomeric SMILES string (Weininger, 1988). We use RDKit (*version 2022.3.5*), an open-source toolkit for cheminformatics to generate the attributed molecular graph for each surfactant. For the graph convolutions, the GINE-operator (Xu et al., 2019; Hu et al., 2020) as implemented in PyTorch Geometric (PyG) (Fey and Lenssen, 2019) is applied with sum being the pooling layer of choice. We use sum pooling as it has been shown to be beneficial for molecular-dependent prediction tasks (Schweidtmann et al., 2023).

4 Results and discussion

In this section, the predictive performance of our GNNs models is evaluated (Section 4.1). Then, we compare our GNN model with predictive CMC models from previous works (Section 4.2). We further analyze the predictive performance for different temperature ranges (Section 4.3) and investigate the influence of the surfactant classes on the CMC predictions (Section 4.4). Finally, the results on selected sugar-based surfactants are presented, which are interesting due to their sustainability aspects (Section 4.5).

4.1 Predictive performance on different temperature and distinct surfactant test sets

We first evaluate the model performance for two different test scenarios (cf. Section 2.2): the *different temperature*, i.e., predicting the CMC of surfactants that have been included in training but at different temperatures, and the *distinct surfactant*, i.e., predicting the CMC at different temperatures of surfactants that have not been used for training at all. Table 2 shows the mean absolute error (MAE), the RMSE, and the mean absolute percentage error (MAPE) on the validation and the test set for both scenarios. Here, we report the performance of the ensemble of GNNs since we found ensemble learning to be beneficial in our previous work (Schweidtmann et al., 2020; Brozos et al., 2024). All reported error metrics refer to the log CMC.

In the *different temperature* scenario, the ensemble of GNNs exhibits an RMSE of 0.173, a MAE of 0.113, a MAPE of 3.561, and a high R^2 of 0.97. For the *distinct surfactant* set, the ensemble of GNNs performs predictions on previously unseen surfactant molecules at single and multiple temperatures with an RMSE of 0.251, an MAE of 0.173, a MAPE of 5.702 and an R^2 of 0.94. Compared to the different

Tab. 2. Summary of GNN ensemble accuracy on the two test set splits for predicting the temperature-dependent CMC on logarithmic scale. The ensembles consist of 40 GNNs. The accuracy is given for the following metrics: MAE = mean absolute error, RMSE = root mean squared error (unit: log CMC), MAPE = mean absolute percentage error (unit %).

	Different temperature				Distinct surfactant			
	RMSE	MAE	MAPE	R^2	RMSE	MAE	MAPE	R^2
GNN ensemble	0.173	0.113	3.561	0.97	0.251	0.173	5.702	0.94

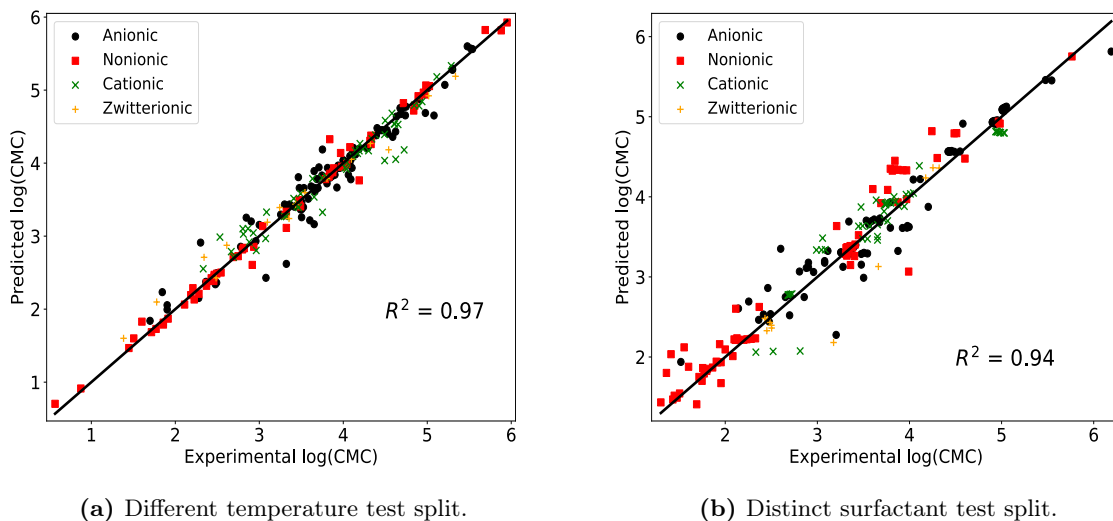


Fig. 4. Parity plots of the ensemble of GNNs on the two test data sets: (a) different temperature and (b) distinct surfactant. Surfactant classes are highlighted with different colors and markers. The logarithm is applied to CMC in μM (base 10).

temperature split, the errors slightly increase, which is expected since predicting the CMC of completely unseen surfactants is more difficult than predicting the CMC of a surfactant, for which CMC values at other temperatures have been included in training the models.

Furthermore, we show parity plots for the predictions of the ensemble of GNN models for both test scenarios, different temperature and distinct surfactant, in Figure 4. For both scenarios, the models show very good agreement between measured and predicted data, as most of the points lie close to the diagonal, resulting in high R^2 scores of 0.97 and 0.94, respectively. We notice only a small number of outliers in both cases; the four points with the highest absolute error (AE) are reported in Figures A10 and A11, respectively. The exact model predictions are directly compared with the experimental measurements in Tables B8 and B9.

Overall, the GNN ensembles provide a high predictive quality, also indicating generalization capabilities to new surfactants not included in the training.

4.2 Comparison with previous works

We further compare the predictive quality of our model to previously developed GNNs from the literature for CMC prediction. An overview of past model predictive performance is given in Table 3. Note that previous works have used different test sets, making a direct comparison difficult. Qin et al. (2021) developed a GNN model for predicting CMCs of surfactant at constant temperature and reported an RMSE of 0.30 on their test set of 22 molecules. This indicates a slightly worse performance on a less diverse test set compared to our GNN model with an RMSE of 0.25 evaluated on 218 different point with 50 distinct molecules. In another recent work, Moriarty et al. (2023) analyzed the GNN model developed by Qin et al. (2021) and reported a combined GNN model with Gaussian Process (GP) with a test RMSE of 0.21, which is slightly lower than our findings. However, the test set was again limited to 22 molecules, which is only about 40% of ours, and therefore may not represent the diversity of surfactant structures used in different practical applications. In their complementary data set, which contains 43 distinct surfactant molecules with some being outside the applicability domain of the model developed by Qin et al. (2021), their best-performing model exhibited an RMSE of 1.32, which is almost six times higher than our findings. In our recent work, we examined the performance of single- and multi-task learning on predicting the CMC and the surface excess concentration (Γ_m) of surfactant monomers with GNNs

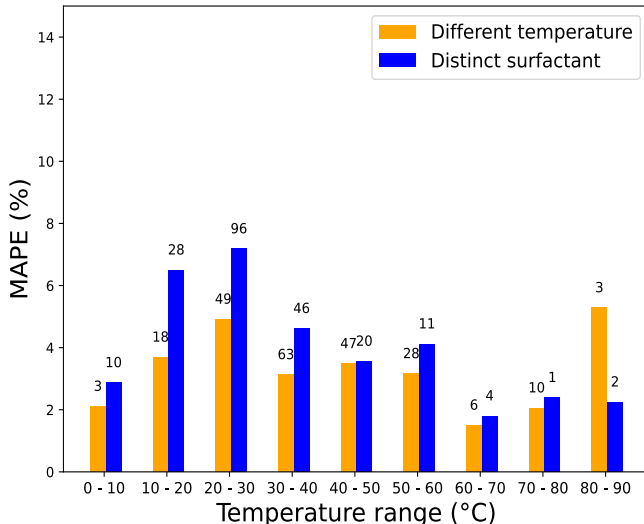
Tab. 3. Comparison of different GNN models for predicting the CMC of surfactants. Dash (–) indicates that values were not provided in previous studies.

Work	Test set size	Temperature dependency	RMSE	R ²
Qin et al. (2021)	22	No	0.30	0.91
Moriarty et al. (2023)	22	No	0.21	–
Moriarty et al. (2023) - complementary set	43	No	1.32	–
Previous work (Brozos et al., 2024)	65	No	0.31	0.94
Current work	218	Yes	0.25	0.94

but without temperature dependency (Brozos et al., 2024). The multi-task GNN exhibited an RMSE of 0.31 and an R² of 0.94 for the CMC, which are slightly worse than our current results. Therefore, we herein increase the predictive quality of GNNs for CMC prediction, although the presented prediction task includes the temperature dependency of the CMC and is thus presumably more challenging. We suspect, that the larger data set used in the present work (1,377 data points compared to 429 data points in our previous work (Brozos et al., 2024)) positively influences the predictive capabilities of the GNNs. Overall, we find our GNN model to perform on a higher level (better test accuracy) with a broader applicability range, more diverse surfactant chemistry, than previous works.

4.3 Analysis of temperature impact on model accuracy

We further examine the model performance for both test sets, different temperature and distinct surfactant, in the whole temperature spectrum. Therefore, we separate the individual temperatures into temperature bins (of 10°C ranges) and we calculate the MAPE in each one. The results are plotted in Figure 5. In most temperature bins, the MAPE is higher on the distinct surfactant split than on the new temperature split, which is expected due to the more challenging prediction task (cf. Section 4.1). We do not observe any temperature range with a significant high error in both test scenarios. As expected, the highest amount of measurements are between 20°C and 30°C.

**Fig. 5.** The mean absolute percentage error (MAPE) on the two test data sets: different temperature (yellow) and distinct surfactant (blue). The mentioned ranges exclude the left limit but include the right limit, for example (0 - 10] and (10 - 20]. The corresponding number of data points for each temperature range are denoted at the top of the respective bars.

We further visualize the temperature dependence of the GNN predicted CMC versus the experimental CMC and the Absolute Percentage Error (APE) for four randomly selected surfactants from the distinct surfactant test set in Figure 6. Please note that different scales of CMC are used in the plots since the order of CMC magnitude varies for different surfactants (cf. Section 2 and Appendix A). The scale of APE in Figure 6d also differs from the rest. Given this wide range of CMC values, Figure 6 shows that the model accurately predicts the order of magnitude of CMC at multiple temperatures. The model also identifies trends for the temperature dependency of the CMC for most cases, e.g., the U-shaped relationship for the two surfactants in Figures 6b-c. For sodium decanoate shown in Figure 6a, the decrease in the CMC for the range of 15-40°C is predicted correctly, but the increase of the CMC up to 55°C is not captured. The highest APE (12%) is observed at Figure 6d at 40°C. While general trends are mostly captured, the model seems to underestimate the temperature effect on the CMC. The lack of high sensitivity to temperature changes may due to the fact that for some surfactants only marginal changes in CMC value are observed at different temperatures, as shown in Figure 2, which are even less pronounced on the logarithmic scale used for model training. Thus, additional training data and further model refinement would be desirable to fully capture the detailed temperature effects in future work.

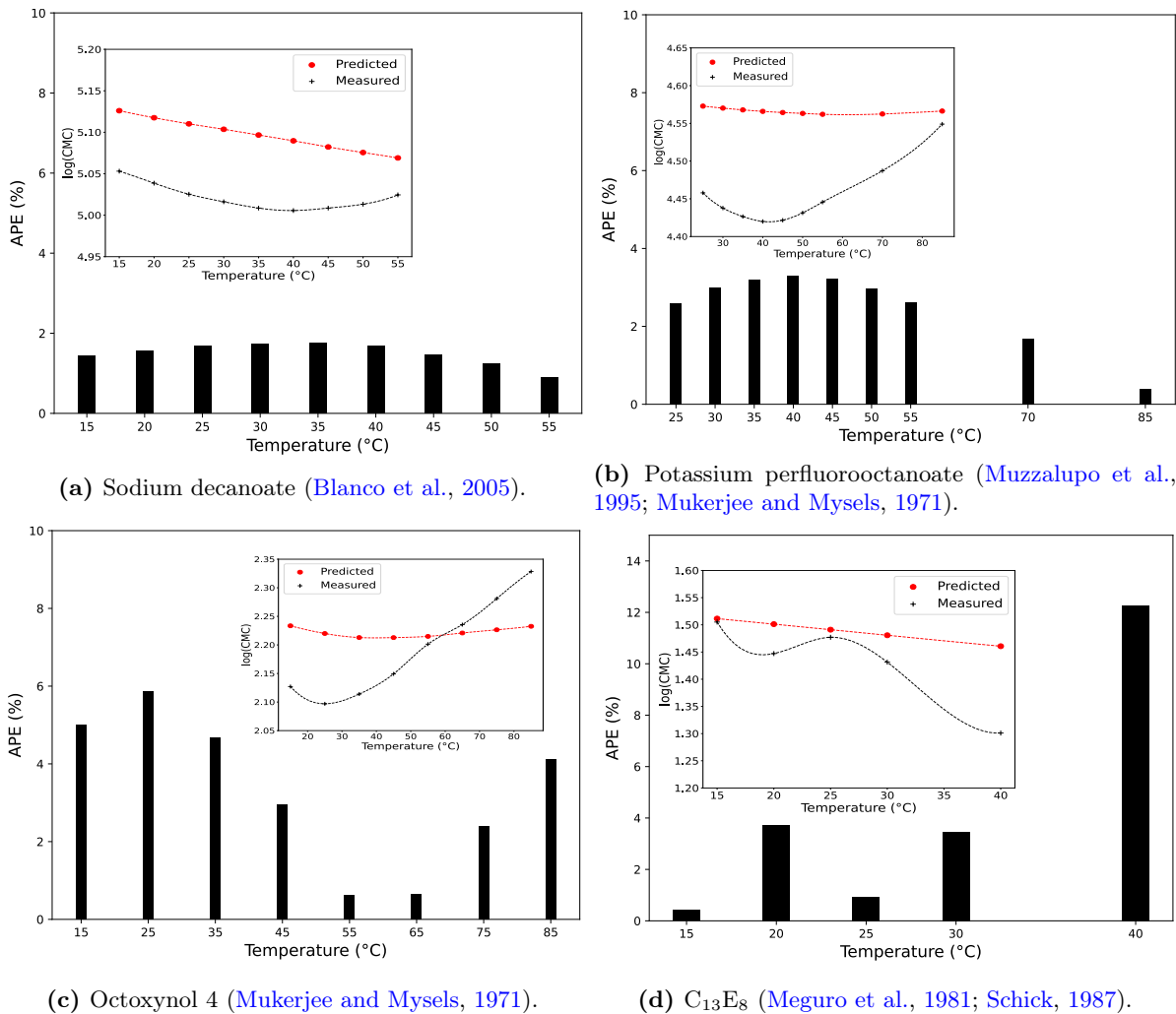


Fig. 6. The GNN predicted versus experimental temperature-dependent performance on four surfactants, part of our test set is shown. Predicted and measured log CMC values are plotted together and connected through a cubic interpolation in the corresponding insets. The logarithm is applied to CMC in μM .

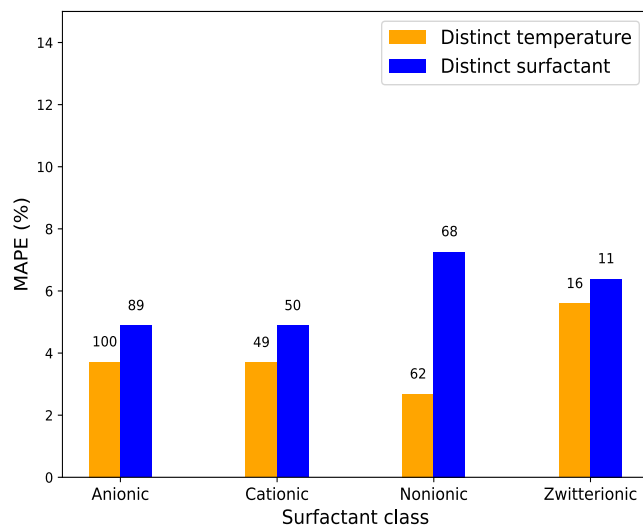


Fig. 7. The mean absolute percentage error (MAPE) per surfactant class on the two test data sets: different temperature (yellow) and distinct surfactant (blue). The corresponding number of data points for each temperature range are denoted at the top of the respective bars.

4.4 Predictive performance per surfactant class

As discussed previously (cf. Section 1), the temperature effect of the CMC is unique for surfactants belonging to different surfactant classes. Thus, from a product development viewpoint, analyzing the results for each class is highly interesting. For example, one would want to identify surfactants and classes that exhibit a lowering of CMC with temperature, since the minimum CMC value and the corresponding temperature may be valuable for different applications (e.g., in laundry applications).

We calculate the MAPE per surfactant class for both test scenarios and report the results in Figure 7. Overall, all surfactant classes demonstrate a MAPE < 8%. Ionic surfactants have a slightly higher error on the distinct surfactant split in comparison to the different temperature split, as unseen surfactant structures are introduced on the test set (cf. Section 2.2). Specifically, anionic and cationic surfactants have the lowest errors in total for the distinct surfactant split. Since they generally exhibit a U-shaped relationship, the model is able to make accurate predictions. Zwitterionics, do not always exhibit the same general CMC-temperature relationship, and therefore decreased model accuracy is observed. For nonionic surfactants, the MAPE is more than doubled in the distinct surfactant split. Here, sugar-based surfactants are also considered. The high complexity of CMC dependency on temperature for such surfactants decreases model accuracy. The model performance on sugar-based surfactants is investigated in the next subsection of this work. Overall, we find model performance to be highly correlated with the number of possible CMC-temperature relationships (U-shaped, monotonically decrease, etc.) in each surfactant class.

4.5 Predictive performance on sugar-based surfactants

Bio-based surfactants and biosurfactants that are comprised of sustainable and natural-based feedstock are of technological importance to personal and home care industries. These often contain either single or multiple sugar groups, which control surfactant properties like foaming, cleansing, etc. Such sugar-based surfactants are complex molecules with many chiral centers on the sugar head. Therefore different anomeric configurations of the sugar groups and hence the entire surfactant structure are possible. In GNNs operating on the molecular graph, which is a 2D representation of the molecule (cf. Section 3.1), such spatial/geometric information is typically solely captured as an atomic feature, thus making it

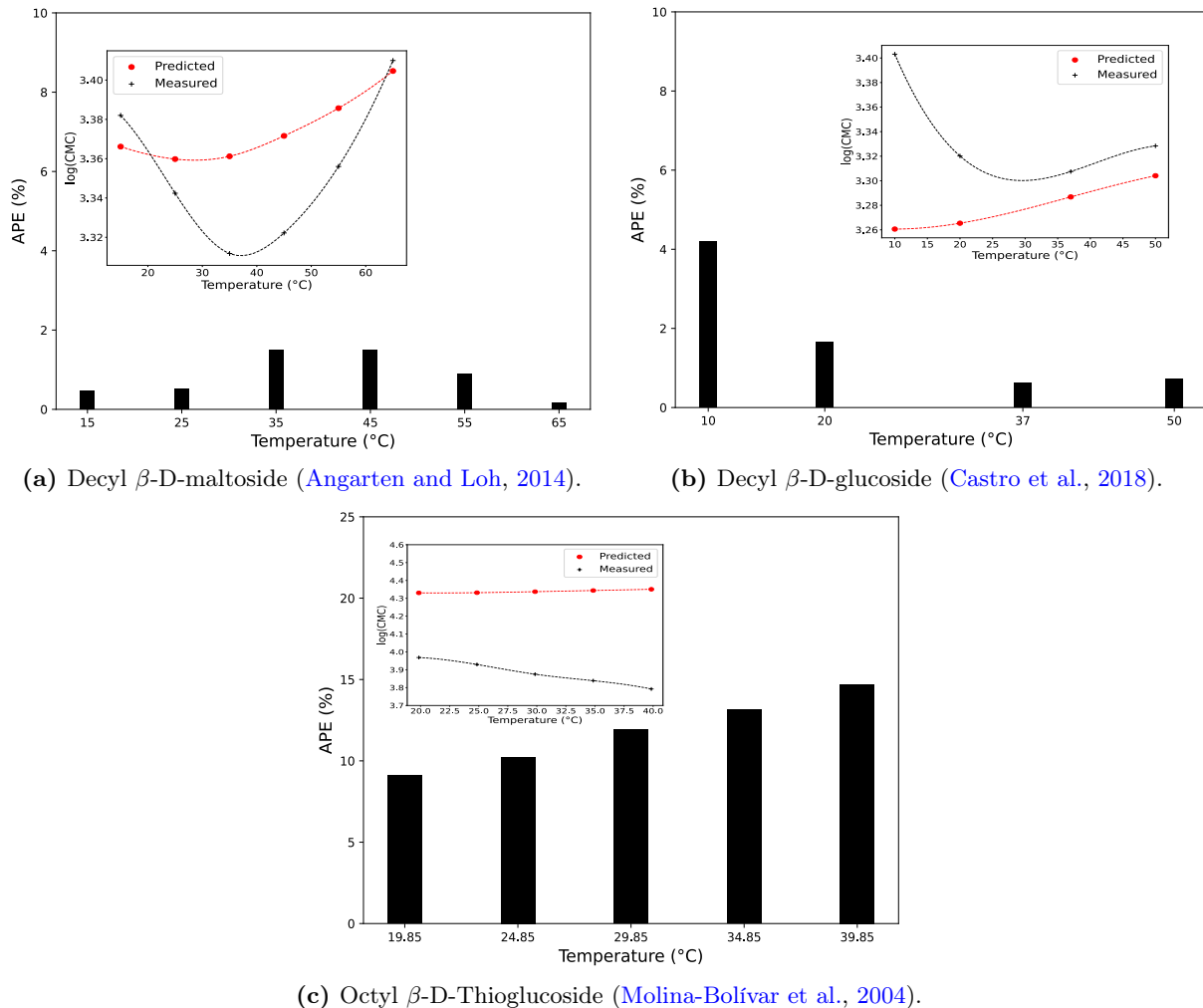


Fig. 8. Ensembled predictions on sugar-based surfactant in the distinct surfactant test set. Predicted and measured log CMC are plotted together and connected through cubic interpolation. The logarithm is applied to CMC in μM . The absolute percentage error (APE) per temperature is also illustrated.

challenging to accurately predict properties of complex sugar-based surfactants. Therefore, we analyze the performance of the model on some selected sugar-based surfactants present in the *distinct surfactant* test set.

We plot the temperature-dependent CMC predictions together with the experimental CMC values from the literature, as well as the APE per temperature in Figure 8. Since absolute (not logarithmic) CMC values are also of interest in practical, industrial applications, we report the absolute predictions on the three sugar-based surfactants in Table B10.

We observe the ability of our model to accurately predict the magnitude of the CMC values for two out of three sugar-based surfactants, namely decyl β -D-glucoside and decyl β -D-maltoside. This is evident by the low APE for these two surfactants across all temperatures. Furthermore, the correct trend of the temperature dependency is identified, except for decyl β -D-maltoside at 10°C . The reason may be the low amount of measurements at this temperature, as shown above in Figure 1. On the other hand, our model fails to accurately predict the real CMC values of octyl β -D-Thioglucoside. As noted by Gaudin et al. (2019), the nature of the linker, i.e., the connection between the carbohydrate and the alkyl chain, impacts the surfactant properties and consequently the CMC. Replacing the ether -O- with thioether -S- linker, leads to incorrect predictions from our model. We note that our data set contains no other

Tab. 4. Comparison between predicted and experimental CMC values for two sugar-based surfactants. The CMC values outside the parenthesis given are the logarithmic ones. The CMC values inside the parenthesis represent the absolute value and are given in mM. Both surfactants are measured at 25°C.

Surfactant	Predicted CMC (μM)	Measured CMC (μM)	Source
Heptyl α -D-mannoside	4.792 (61.937)	4.49 (30.6)	(Gaudin et al., 2019)
Heptyl α -D-galactoside	4.795 (62.373)	4.512 (32.5)	(Gaudin et al., 2019)

sugar-based surfactant with thioether as the linker. Thus, expanding the data set further with more experimental data on sugar-based surfactants would improve the predictions of our model.

We are further interested in the effect of anomeric configuration and chirality centers of sugar-based surfactants on the CMC predictions. Since all previously discussed sugar-based surfactants had an β anomeric configuration, we analyze the model performance on heptyl- α -D-mannoside and heptyl- α -D-galactoside at a single temperature. The calculated and measured CMC values are given in Table 4. We observe a relatively high absolute error for both surfactants, namely 0.306 and 0.283 respectively. Note here that the overall MAE was found to be 0.173 (cf. Section 4.1). The most often present sugar-based surfactants on our database are of the n-alkanoyl- β -D-glucoside type. In comparison with them, both surfactants exhibit structural differences in their anomeric configuration and chirality centers of the sugar head. Specifically, our training data set contains only two surfactants with mannoside and three surfactants with galactoside as the polar head. Given the limited amount of similarly structured surfactants in the training set, the model provides acceptable CMC predictions but with an above-average error compared to the overall MAPE of the distinct surfactant test set. To enable the GNN to additionally learn different structures/linkers in sugar-based surfactants, systematic CMC data on these surfactants should be provided in the future.

5 Conclusion

We develop a GNN model for the prediction of the temperature-dependent CMC of surfactants. For this, we first assemble a data set with 1,377 CMC measurements at multiple temperatures ranging from 0°C to 90°C for 492 unique surfactants covering all surfactant classes, i.e., anionic, cationic, zwitterionic, and nonionic surfactants. We then use this data set to train an ensemble of GNN models directly on the molecular graph of the surfactants and the temperature information, thereby enabling the prediction of temperature dependency of the CMC, a key interest in personal and home care applications.

The GNN model exhibits very high predictive quality. Specifically, the model shows accurate predictions for surfactants included in the training but at a different temperature and for surfactants not seen during training at all, thus generalizing to new surfactants. Model performance remained constant throughout all temperature ranges but varied per surfactant class. The GNN model also outperforms previously developed data-driven models for predicting the CMC at constant temperature. Detailed temperature dependencies are not fully captured by the model yet, i.e., the model underestimates the sensitivity of the CMC to changes in the temperature, demonstrating the need for additional temperature-dependent CMC data and model refinement.

We specifically investigate sustainably sourced sugar-based surfactants. The GNN model incorporates anomeric and chirality information into the feature vector and can thus distinguish between different anomers and isomers. The GNN provides accurate predictions of the CMC at multiple temperatures for two exemplary sugar-based surfactants but also shows limitations in differentiating ether (-O-) and thioether (-S-) linker in a third selected sugar-based surfactant. Further evaluation of the anomeric and chirality information effect on the model performance showed an above-average error and model limitations in distinguishing between different chiral centers on the sugar head. Yet, the model accurately predicts the order of magnitude of the temperature-dependent CMC values for sugar-based surfactants.

Future work should focus on acquiring additional temperature-dependent CMC data for model training. To account for the CMC relation to the geometry of the molecular structure, which is particularly relevant for sugar-based surfactants, geometric GNNs that consider atomic coordinates could be investigated. Also, extending the GNN model to incorporate pH conditions and defining the validity domain of

the model would be insightful extensions. Finally, obtaining chemical intuition on how the model performs predictions by using explainable AI methods could help to better understand surfactant self-aggregation.

Acknowledgments

The BASF authors (C. Brozos, S. Bhattacharya, E. Akanny, and C. Kohlmann) were funded by the BASF Personal Care and Nutrition GmbH. J. G. Rittig and A. Mitsos acknowledge funding from the Deutsche Forschungsgemeinschaft (DFG, German Research Foundation) – 466417970 – within the Priority Programme “SPP 2331: Machine Learning in Chemical Engineering”. Additionally, J. G. Rittig acknowledges the support of the Helmholtz School for Data Science in Life, Earth and Energy (HDS-LEE).

Data availability

All Python scripts and the test data used in this work are available as open-source in our [GitHub repository](#).

Author contribution

Christoforos Brozos: Conceptualization, Methodology, Software, Data curation, Validation, Formal analysis, Writing - Original Draft, Writing - Review & Editing, Visualization

Jan G. Rittig: Conceptualization, Methodology, Software, Formal analysis, Writing - Review & Editing

Sandip Bhattacharya: Conceptualization, Methodology, Formal analysis, Supervision, Writing - Review & Editing

Elie Akanny: Conceptualization, Methodology, Experimental methodology & measurements, Writing - Review & Editing

Christina Kohlmann: Writing - Review & Editing, Supervision, Funding acquisition

Alexander Mitsos: Writing - Review & Editing, Supervision, Funding acquisition

Bibliography

- Abooli, D. and Soleimani, R. (2023). Structure-based modeling of critical micelle concentration (cmc) of anionic surfactants in brine using intelligent methods. *Scientific Reports*, 13(1):13361.
- Adams, K., Pattanaik, L., and Coley, C. W. (2021). Learning 3d representations of molecular chirality with invariance to bond rotations. *ArXiv*, abs/2110.04383.
- Adu, S. A., Naughton, P. J., Marchant, R., and Banat, I. M. (2020). Microbial biosurfactants in cosmetic and personal skincare pharmaceutical formulations. *Pharmaceutics*, 12.
- Angarten, R. G. and Loh, W. (2014). Thermodynamics of micellization of homologous series of alkyl mono and di-glucosides in water and in heavy water. *The Journal of Chemical Thermodynamics*, 73:218–223. Special issue honoring Professor Manuel Ribeiro da Silva.
- Blanco, E., González-Pérez, A., Ruso, J. M., Pedrido, R., Prieto, G., and Sarmiento, F. (2005). A comparative study of the physicochemical properties of perfluorinated and hydrogenated amphiphiles. *Journal of Colloid and Interface Science*, 288(1):247–260.
- Breiman, L. (1996). Bagging predictors. *Machine Learning*, 24(2):123–140.
- Brinatti, C., Mello, L. B., and Loh, W. (2014). Thermodynamic study of the micellization of zwitterionic surfactants and their interaction with polymers in water by isothermal titration calorimetry. *Langmuir*, 30(21):6002–6010.
- Brozos, C., Rittig, J. G., Bhattacharya, S., Akanny, E., Kohlmann, C., and Mitsos, A. (2024). Graph neural networks for surfactant multi-property prediction.
- Buterez, D., Janet, J. P., Kiddle, S. J., Oglic, D., and Liò, P. (2023). Modelling local and general quantum mechanical properties with attention-based pooling. *Communications Chemistry*, 6(1):262.
- Cangea, C., Veličković, P., Jovanović, N., Kipf, T., and Liò, P. (2018). Towards sparse hierarchical graph classifiers.
- Castro, G., Garrido, P. F., Amigo, A., and Brocos, P. (2018). Boosting the use of thermoacoustimetry in micellization thermodynamics studies by easing an objective determination of the cmc. *Fluid Phase Equilibria*, 478:1–13.
- Chen, L.-J., Lin, S., and Huang, C.-C. (1998). Effect of hydrophobic chain length of surfactants on enthalpy-entropy compensation of micellization. *Journal of Physical Chemistry B*, 102:4350–4356.
- Cheng, C.-j., Qu, G.-m., Wei, J.-j., Yu, T., and Ding, W. (2012). Thermodynamics of micellization of sulfobetaine surfactants in aqueous solution. *Journal of Surfactants and Detergents*, 15(6):757–763.
- Dietterich, T. G. (2000). Ensemble methods in machine learning. In *Proceedings of the First International Workshop on Multiple Classifier Systems*, MCS '00, page 1–15, Berlin, Heidelberg. Springer-Verlag.
- Drakontis, C. E. and Amin, S. (2020). Biosurfactants: Formulations, properties, and applications. *Current Opinion in Colloid & Interface Science*, 48:77–90. Formulations and Cosmetics.
- Farias, C. B. B., Almeida, F. C., Silva, I. A., Souza, T. C., Meira, H. M., de Cássia F. Soares da Silva, R., Luna, J. M., Santos, V. A., Converti, A., Banat, I. M., and Sarubbo, L. A. (2021). Production of green surfactants: Market prospects. *Electronic Journal of Biotechnology*, 51:28–39.
- Fey, M. and Lenssen, J. E. (2019). Fast graph representation learning with pytorch geometric. *ArXiv*, abs/1903.02428.
- Fu, D., Gao, X., Huang, B., Wang, J., Sun, Y., Zhang, W., Kan, K., Zhang, X., Xie, Y., and Sui, X. (2019). Micellization, surface activities and thermodynamics study of pyridinium-based ionic liquid surfactants in aqueous solution. *RSC Adv.*, 9:28799–28807.

- Galgano, P. D. and El Seoud, O. A. (2010). Micellar properties of surface active ionic liquids: A comparison of 1-hexadecyl-3-methylimidazolium chloride with structurally related cationic surfactants. *Journal of Colloid and Interface Science*, 345(1):1–11.
- Ganaie, M., Hu, M., Malik, A., Tanveer, M., and Suganthan, P. (2022). Ensemble deep learning: A review. *Engineering Applications of Artificial Intelligence*, 115:105151.
- Gaudin, T., Lu, H., Fayet, G., Berthault-Drelich, A., Rotureau, P., Pourceau, G., Wadouachi, A., Van Hecke, E., Nesterenko, A., and Pezron, I. (2019). Impact of the chemical structure on amphiphilic properties of sugar-based surfactants: A literature overview. *Advances in Colloid and Interface Science*, 270:87–100.
- Gaudin, T., Rotureau, P., Pezron, I., and Fayet, G. (2016). New qspr models to predict the critical micelle concentration of sugar-based surfactants. *Ind. Eng. Chem. Res.*, 55(45):11716–11726.
- Ghezzi, M., Pescina, S., Padula, C., Santi, P., Del Favero, E., Cantù, L., and Nicoli, S. (2021). Polymeric micelles in drug delivery: An insight of the techniques for their characterization and assessment in biorelevant conditions. *Journal of Controlled Release*, 332:312–336.
- Gilmer, J., Schoenholz, S. S., Riley, P. F., Vinyals, O., and Dahl, G. E. (2017). Neural message passing for quantum chemistry.
- González-Pérez, A., Ruso, J. M., Romero, M. J., Blanco, E., Prieto, G., and Sarmiento, F. (2005). Application of thermodynamic models to study micellar properties of sodium perfluoroalkyl carboxylates in aqueous solutions. *Chemical Physics*, 313(1):245–259.
- Hamilton, W. L. (2020). *Graph representation learning*. Morgan & Claypool Publishers.
- Hamilton, W. L., Ying, R., and Leskovec, J. (2018). Inductive representation learning on large graphs.
- Hu, J., Zhang, X., and Wang, Z. (2010). A review on progress in qspr studies for surfactants. *International journal of molecular sciences*, 11:1020–47.
- Hu, W., Liu, B., Gomes, J., Zitnik, M., Liang, P., Pande, V., and Leskovec, J. (2020). Strategies for pre-training graph neural networks.
- Jahan, R., Bodratti, A. M., Tsianou, M., and Alexandridis, P. (2020). Biosurfactants, natural alternatives to synthetic surfactants: Physicochemical properties and applications. *Advances in Colloid and Interface Science*, 275:102061.
- Katritzky, A. R., Pacureanu, L. M., Slavov, S. H., Dobchev, D. A., and Karelson, M. (2008). Qspr study of critical micelle concentrations of nonionic surfactants. *Ind. Eng. Chem. Res.*, 47(23):9687–9695.
- Klevens, H. B. (1953). Structure and aggregation in dilute solution of surface active agents. *Journal of the American Oil Chemists Society*, 30(2):74–80.
- Kroll, P., Benke, J., Enders, S., Brandenbusch, C., and Sadowski, G. (2022). Influence of temperature and concentration on the self-assembly of nonionic surfactants: A light scattering study. *ACS Omega*, 7(8):7057–7065.
- Kumar, A. and Mandal, A. (2019). Critical investigation of zwitterionic surfactant for enhanced oil recovery from both sandstone and carbonate reservoirs: Adsorption, wettability alteration and imbibition studies. *Chemical Engineering Science*, 209:115222.
- Lindman, B., Medronho, B., and Karlström, G. (2016). Clouding of nonionic surfactants. *Current Opinion in Colloid & Interface Science*, 22:23–29.
- Massarweh, O. and Abushaikha, A. S. (2020). The use of surfactants in enhanced oil recovery: A review of recent advances. *Energy Reports*, 6:3150–3178.

- Mattei, M., Kontogeorgis, G. M., and Gani, R. (2013). Modeling of the critical micelle concentration (cmc) of nonionic surfactants with an extended group-contribution method. *Ind. Eng. Chem. Res.*, 52(34):12236–12246.
- Meguro, K., Takasawa, Y., Kawahashi, N., Tabata, Y., and Ueno, M. (1981). Micellar properties of a series of octaethyleneglycol-n-alkyl ethers with homogeneous ethylene oxide chain and their temperature dependence. *Journal of Colloid and Interface Science*, 83:50–56.
- Molina-Bolívar, J. A., Aguiar, J., Peula-García, J. M., and Ruiz, C. C. (2004). Surface activity, micelle formation, and growth of n-octyl- β -d-thioglucopyranoside in aqueous solutions at different temperatures. *J. Phys. Chem. B*, 108(34):12813–12820.
- Moriarty, A., Kobayashi, T., Salvalaglio, M., Angeli, P., Striolo, A., and McRobbie, I. (2023). Analyzing the accuracy of critical micelle concentration predictions using deep learning. *J. Chem. Theory Comput.*, 19(20):7371–7386.
- Mukerjee, P. and Mysels, K. J. (1971). Critical micelle concentrations of aqueous surfactant systems. Technical report, National Standard reference data system.
- Muzzalupo, R., Ranieri, G. A., and La Mesa, C. (1995). Solution properties of alkali metal perfluoroalkanoates. *Colloids and Surfaces A: Physicochemical and Engineering Aspects*, 104(2):327–336.
- Myers, D. (August 2020). *Surfactant Science and Technology, 4th Edition*. John Wiley & Sons, Ltd.
- Nitschke, M. and Costa, S. (2007). Biosurfactants in food industry. *Trends in Food Science & Technology*, 18(5):252–259.
- Okawauchi, M., Hagio, M., Ikawa, Y., Sugihara, G., Murata, Y., and Tanaka, M. (1987). A light-scattering study of temperature effect on micelle formation of n-alkanoyl-n-methylglucamines in aqueous solution. *Bulletin of the Chemical Society of Japan*, 60(8):2719–2725.
- Omar, A.-A. M. A. and Abdel-Khalek, N. A. (1998). Surface and thermodynamic parameters of some cationic surfactants. *J. Chem. Eng. Data*, 43(1):117–120.
- Paula, S., Sues, W., Tuchtenhagen, J., and Blume, A. (1995). Thermodynamics of micelle formation as a function of temperature: A high sensitivity titration calorimetry study. *The Journal of Physical Chemistry*, 99(30):11742–11751.
- Perger, T.-M. and Bešter-Rogač, M. (2007). Thermodynamics of micelle formation of alkyltrimethylammonium chlorides from high performance electric conductivity measurements. *Journal of Colloid and Interface Science*, 313(1):288–295.
- Prasad, M., Chakraborty, I., Rakshit, A. K., and Moulik, S. P. (2006). Critical evaluation of micellization behavior of nonionic surfactant mega 10 in comparison with ionic surfactant tetradecyltriphenylphosphonium bromide studied by microcalorimetric method in aqueous medium. *J. Phys. Chem. B*, 110(20):9815–9821.
- Qin, S., Jin, T., Van Lehn, R. C., and Zavala, V. M. (2021). Predicting critical micelle concentrations for surfactants using graph convolutional neural networks. *The journal of physical chemistry. B*, 125:10610–10620.
- Rittig, J. G., Ben Hicham, K., Schweidtmann, A. M., Dahmen, M., and Mitsos, A. (2023a). Graph neural networks for temperature-dependent activity coefficient prediction of solutes in ionic liquids. *Computers and Chemical Engineering*, 171:108153.
- Rittig, J. G., Felton, K. C., Lapkin, A. A., and Mitsos, A. (2023b). Gibbs–duhem-informed neural networks for binary activity coefficient prediction. *Digital Discovery*, 2:1752–1767.
- Rittig, J. G., Gao, Q., Dahmen, M., Mitsos, A., and Schweidtmann, A. M. (2022). Graph neural networks for the prediction of molecular structure-property relationships.

- Rosen, M. and Kunjappu, J. (2012). *Surfactants and Interfacial Phenomena: Rosen/Surfactants 4E*. John Wiley & Sons, Ltd.
- Ruiz, C. C. (2008). *Sugar-based surfactants: fundamentals and applications*, volume 143. CRC Press.
- Sanchez Medina, E. I., Linke, S., Stoll, M., and Sundmacher, K. (2022). Graph neural networks for the prediction of infinite dilution activity coefficients. *Digital Discovery*, 1:216–225.
- Sanchez Medina, E. I., Linke, S., Stoll, M., and Sundmacher, K. (2023). Gibbs–helmholtz graph neural network: capturing the temperature dependency of activity coefficients at infinite dilution. *Digital Discovery*, 2:781–798.
- Schick, M. J. (1987). *Nonionic Surfactants: Physical Chemistry*. Marcel Dekker, Inc., New York and Basel.
- Schweidtmann, A. M., Rittig, J. G., König, A., Grohe, M., Mitsos, A., and Dahmen, M. (2020). Graph neural networks for prediction of fuel ignition quality. *Energy & Fuels*, 34(9):11395–11407.
- Schweidtmann, A. M., Rittig, J. G., Weber, J. M., Grohe, M., Dahmen, M., Leonhard, K., and Mitsos, A. (2023). Physical pooling functions in graph neural networks for molecular property prediction. *Computers & Chemical Engineering*, 172:108202.
- Seddon, D., Müller, E. A., and Cabral, J. T. (2022). Machine learning hybrid approach for the prediction of surface tension profiles of hydrocarbon surfactants in aqueous solution. *Journal of Colloid and Interface Science*, 625:328–339.
- Shaban, S. M., Kang, J., and Kim, D.-H. (2020). Surfactants: Recent advances and their applications. *Composites Communications*, 22:100537.
- Shinoda, K. and Hirai, T. (1977). Ionic surfactants applicable in the presence of multivalent cations. physicochemical properties. *The Journal of Physical Chemistry*, 81:1842–1845.
- Simonovsky, M. and Komodakis, N. (2017). Dynamic edge-conditioned filters in convolutional neural networks on graphs.
- Su, H., Wang, F., Ran, W., Zhang, W., Dai, W., Wang, H., Anderson, C. F., Wang, Z., Zheng, C., Zhang, P., Li, Y., and Cui, H. (2020). The role of critical micellization concentration in efficacy and toxicity of supramolecular polymers. *Proceedings of the National Academy of Sciences of the United States of America*, 117:4518–4526.
- Szűts, A. and Szabó-Révész, P. (2012). Sucrose esters as natural surfactants in drug delivery systems—a mini-review. *International Journal of Pharmaceutics*, 433(1):1–9.
- Tadros, T. (2005). *Surfactants in Personal Care and Cosmetics*, chapter 12, pages 399–432. John Wiley & Sons, Ltd.
- Thiruvengadam, S., Murphy, M., Tan, J. S., and Miller, K. (2020). A generalized theoretical model for the relationship between critical micelle concentrations, pressure, and temperature for surfactants. *Journal of Surfactants and Detergents*, 23(2):273–303.
- Thompson, C. J., Ainger, N., Starck, P., Mykhaylyk, O. O., and Ryan, A. J. (2023). Shampoo science: A review of the physicochemical processes behind the function of a shampoo. *Macromolecular Chemistry and Physics*, 224(3):2200420.
- Veličković, P., Cucurull, G., Casanova, A., Romero, A., Liò, P., and Bengio, Y. (2018). Graph attention networks.
- Vieira, I. M. M., Santos, B. L. P., Ruzene, D. S., and Silva, D. P. (2021). An overview of current research and developments in biosurfactants. *Journal of Industrial and Engineering Chemistry*, 100:1–18.

- Vinyals, O., Bengio, S., and Kudlur, M. (2016). Order matters: Sequence to sequence for sets.
- Vu, T.-S., Ha, M.-Q., Nguyen, D.-N., Nguyen, V.-C., Abe, Y., Tran, T., Tran, H., Kino, H., Miyake, T., Tsuda, K., and Dam, H.-C. (2023). Towards understanding structure-property relations in materials with interpretable deep learning. *npj Computational Materials*, 9(1):215.
- Wang, Y., Yan, F., Jia, Q., and Wang, Q. (2018). Quantitative structure-property relationship for critical micelles concentration of sugar-based surfactants using norm indexes. *Journal of Molecular Liquids*, 253:205–210.
- Weininger, D. (1988). Smiles, a chemical language and information system. 1. introduction to methodology and encoding rules. *J. Chem. Inf. Comput. Sci.*, 28(1):31–36.
- Wu, Z., Pan, S., Chen, F., Long, G., Zhang, C., and Yu, P. S. (2021). A comprehensive survey on graph neural networks. *IEEE Transactions on Neural Networks and Learning Systems*, 32(1):4–24.
- Xu, J., Cao, F., Li, T., Zhang, S., Gao, C., and Wu, Y. (2016). Itaconic acid based surfactants: I. synthesis and characterization of sodium n-octyl sulfoitaconate diester anionic surfactant. *Journal of Surfactants and Detergents*, 19(2):373–379.
- Xu, K., Hu, W., Leskovec, J., and Jegelka, S. (2019). How powerful are graph neural networks?
- Yang, K., Swanson, K., Jin, W., Coley, C., Eiden, P., Gao, H., Guzman-Perez, A., Hopper, T., Kelley, B., Mathea, M., Palmer, A., Settels, V., Jaakkola, T., Jensen, K., and Barzilay, R. (2019). Analyzing learned molecular representations for property prediction. *Journal of Chemical Information and Modeling*, 59(8):3370–3388. PMID: 31361484.
- Zhou, J., Cui, G., Hu, S., Zhang, Z., Yang, C., Liu, Z., Wang, L., Li, C., and Sun, M. (2020). Graph neural networks: A review of methods and applications. *AI Open*, 1:57–81.

A Figures

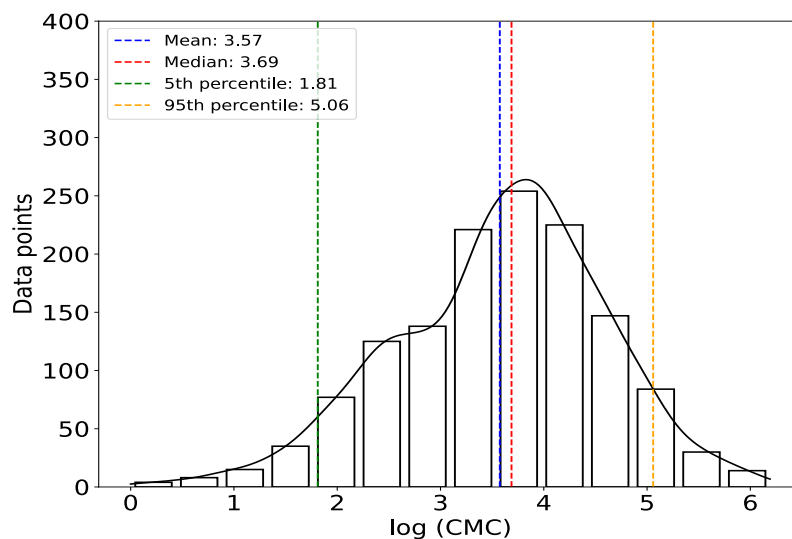


Fig. A9. Statistical overview of the CMC. The logarithm is applied to CMC in μM .

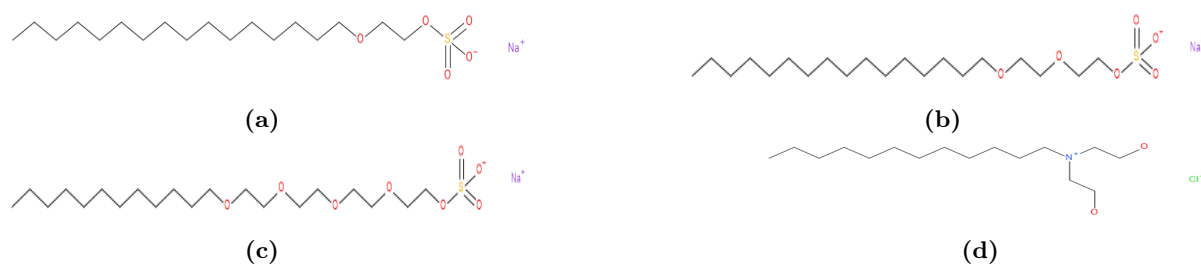


Fig. A10. Outliers of the ensembled GNN model in different temperature split. The first three of them belong to anionic class and the last one is cationic.

B Tables

Tab. B5. Atom features used in the molecular graph representation. All features are implemented as one-hot-encoding.

Feature	Description	Dimension
atom type	atom type (C, N, O, S, F, Cl, Br, Na, I, B, K, H, Li)	13
is in a ring	if the atom is part of a ring	1
is aromatic	if the atom is part of an aromatic system	1
hybridization	sp ² , sp ³	2
chirality	unspecified, clockwise, counter clockwise	3
charge	formal charge of the atom (-1,0,1)	3
# bonds	number of bonds the atom is involved in	5
# Hs	number of bonded hydrogen atoms	5
Total		33

Tab. B6. Edge features used in the molecular graph representation. All features are implemented as one-hot-encoding.

Feature	Description	Dimension
bond type	single, double, or atomatic	3
is in a ring	is the bond part of a ring ?	1
conjugated	is the bond conjugated ?	1
stereo	none or E/Z	3
Total		8

Tab. B7. Hyperparameters of the GNN model investigated through a grid search. The hyperparameter dimensions refers to the size of the molecular fingerprint and the size of the MLP.

Hyperparameter	Range	Optimized geometry
Graph convolutional layers	(1, 2)	1
Graph convolutional type	(NNConv, GINEConv)	GINEConv
Usage of GRU	(True, False)	False
Initial learning rate	(0.005, 0.01, 0.05)	0.005
Batch size	(16, 32, 64)	32
Dimensions	(64, 128)	128
Number of MLP layers	3	3
Activation function	ReLU	ReLU
Maximum epochs	300	300
Early stopping patience	60	60
Learning rate decay	0.8	0.8
Patiance	3	3
Optimizer	Adam	Adam

Tab. B8. Comparison of predicted vs measured CMC values of the 4 outlier for the different temperature split. The data source is provided.

	Different temperature test set			
	Pred. CMC (mM)	Meas. CMC (mM)	Source	Temp. (°C)
Outlier 1	0.42	2.1	(Mukerjee and Mysels, 1971)	25
Outlier 2	0.27	1.2	(Mukerjee and Mysels, 1971)	25
Outlier 3	0.82	0.2	(Myers, 2020)	25
Outlier 4	11.28	42.1	(Omar and Abdel-Khalek, 1998)	34.85

Tab. B9. Comparison of predicted vs measured CMC values of the 4 outlier for the distinct surfactant test set. The data source is provided.

	Distinct surfactant test set			
	Pred. CMC (mM)	Meas. CMC (mM)	Source	Temp. (°C)
Outlier 1	0.15	1.5	(Rosen and Kunjappu, 2012)	25
Outlier 2	0.19	1.6	(Shinoda and Hirai, 1977)	25
Outlier 3	1.17	9.8	(Mattei et al., 2013)	25
Outlier 4	2.24	0.4	(Xu et al., 2016)	20

Tab. B10. Comparison for predicted vs measured CMC values (in mM) of the 3 selected sugar-based surfactants present in the distinct surfactant test set. ^α At 37°C.

Temp. (°C)	Decyl β -D-maltoside		Decyl β -D-glucoside		Octyl β -D-Thioglucoside	
	Pred.	Meas.	Pred.	Meas.	Pred.	Meas.
10			1.82	2.53		
15	2.32	2.41				
20			1.84	2.09	21.4	9.3
25	2.29	2.2			21.45	8.5
30					21.73	7.5
35	2.3	2.05	1.94 ^α	2.03 ^α	22.06	6.9
40					22.42	6.2
45	2.35	2.1				
50			2.01	2.13		
55	2.43	2.27				
65	2.53	2.57				